

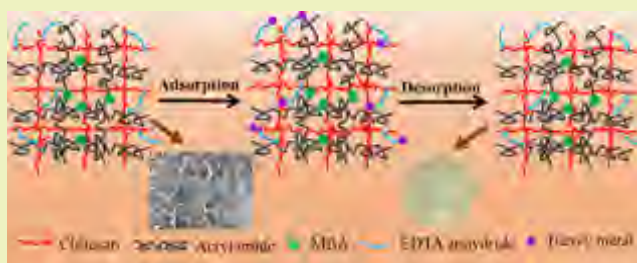
Efficient Removal of Heavy Metal Ions with An EDTA Functionalized Chitosan/Polyacrylamide Double Network Hydrogel

Jianhong Ma,^{†,‡} Guiyin Zhou,[§] Lin Chu,[§] Yutang Liu,^{*,†,‡,§} Chengbin Liu,[§] Shenglian Luo,[§] and Yuanfeng Wei[§]

[†]College of Environmental Science and Engineering and [‡]Key Laboratory of Environmental Biology and Pollution Control, [§]State Key Laboratory of Chemo/Biosensing and Chemometrics, Hunan University, Lushan South Road, Yuelu District, Changsha 410082, P. R. China

Supporting Information

ABSTRACT: A ethylenediaminetetra-acetic acid (EDTA) cross-linked chitosan and *N,N*-methylenebis(acrylamide) (MBA) cross-linked polyacrylamide based double network hydrogel was successfully synthesized via a two-step method and then employed for heavy metal ion adsorption. Various adsorption conditions, such as pH, ionic strength, adsorbent dosage, and contact time were investigated. CTS/PAM gel have a theoretical maximum Cd(II), Cu(II), and Pb(II) sorption capacities of 86.00, 99.44, and 138.41 mg/g, respectively, at experimental conditions. The adsorption process of CTS/PAM gel on the heavy metal ion was identified to be endothermic and follows an ion-exchange reaction. The application of this gel adsorbent was demonstrated using practical industrial effluent. We found that it could effectively treat practical wastewater with all kinds of heavy metals. At an adsorbent dosage of 8 g/L, the total metal ions concentration declined from 448.5 to 5.0 mg/L. Simultaneously, the CTS/PAM gel exhibited remarkable mechanical strength and good recyclability. This study shows that CTS/PAM gel offers great potential for practical application in the removal of heavy metal ions from contaminated aquatic systems.



KEYWORDS: Hydrogel adsorbent, Macroporous network, Practical wastewater, Reusability

INTRODUCTION

Much attention has been paid to water security¹ and water scarcity² for a time as water is widely regarded as the most essential natural resource. What's more, water pollution has become one of the main reasons for poor water quality. Inappropriate discharges of wastewater from industrial processes, such as mining, smelting, and electronics and battery manufacturing, have lead to the release of heavy metal ions into aquatic systems. Heavy metal contamination is extremely harmful to both public health and aquatic life because of its notorious influence on biological systems. Many techniques have been widely used to remove heavy metal ions from aqueous streams, such as precipitation,³ adsorption,⁴ oxidation,⁵ nanofiltration,⁶ and so on, and among these techniques, adsorption has been viewed as a promising water treatment technology for its easy operation, higher cost effectiveness, and diversity of adsorbents. In the last several decades, the adsorption of heavy metal ions on various materials such as nanoparticles,⁷ biosorbents,⁸ and metal–organic frameworks⁹ has been widely studied. However, certain limitations exist in most materials, such as complex preparation, tedious separation, and low reusability, and thus, adsorption cannot achieve a good status at commercial levels.¹⁰

Hydrogels, a three-dimensional “soft-and-wet” material, who can undergo large deformations in volume by exuding or

absorbing water and its swelling behavior and water permeability are highly correlated.¹¹ In addition, the high water content of hydrogels allows more rapid ion penetration that helps to form combinations of functional units on gels.¹² Nevertheless, certain flaws exist in conventional hydrogels that restrict their extensive use for practical applications, for example, low mechanical strength and poor recoverability.¹³ Therefore, many efforts have been devoted to the exploitation of higher mechanical properties hydrogels recent years.¹⁴ Double-network (DN) hydrogel, a hydrogel based on two interpenetrating and cross-linked polymer networks, can enhance the maximum extension, fracture energy, and retention of material properties of hydrogels.¹⁵ With the high mechanic strength, the spent DN gel adsorbent could be easily separated and recovered from aqueous solution. Therefore, the DN hydrogel gives a new concept as a promising adsorbent for wastewater treatment.

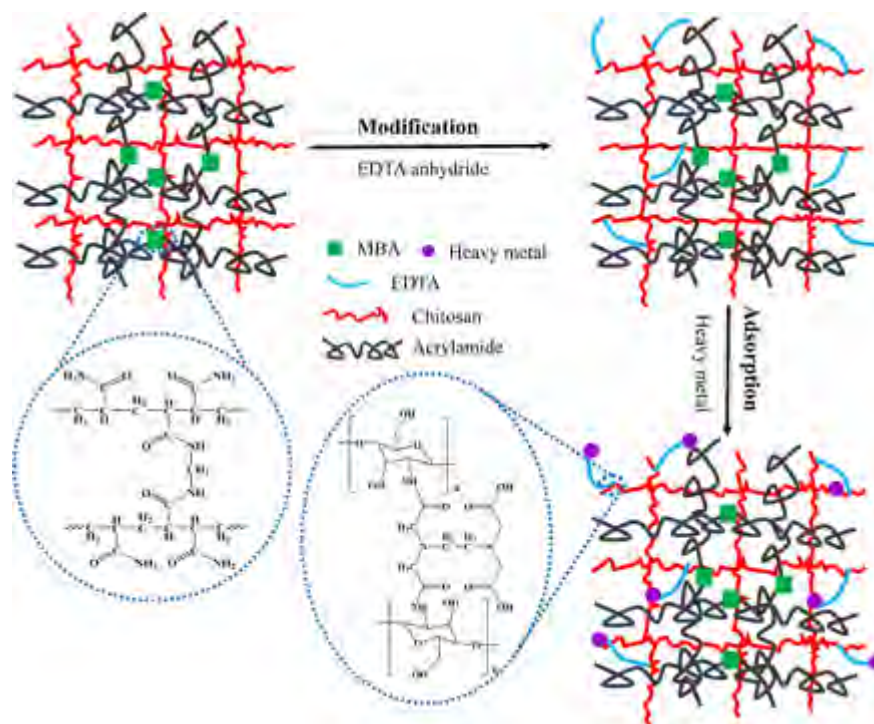
The objective of this study was to establish an innovative chitosan (CTS) and acrylamide (PAM) based DN hydrogel adsorbent for heavy metal removal. As the product of the deacetylation of chitin, chitosan can be easily characterized as a

Received: September 10, 2016

Revised: November 13, 2016

Published: November 21, 2016

Scheme 1. Schematic Representation of CTS/PAM Gel Synthesis



promising adsorption material for the widespread abundance and the existence of modifiable positions in its chemical structure.^{16,17} Until now, many works about chitosan and polyacrylamide have been published.^{18–24} However, details about an ethylenediaminetetra-acetic acid (EDTA) cross-linked chitosan and *N,N*-methylenebis(acrylamide) (MBA) cross-linked polyacrylamide based double network hydrogel have not been published. Thus, in this study, EDTA cross-linked chitosan was introduced into the synthesis of DN hydrogel as the first network,²⁵ and the second network was formed by polyacrylamide chains through MBA cross-links. The polyacrylamide network performed as the ductile and tough second network which can bear stress and reconstruct network structure.²⁶ EDTA not only performed as the cross-linker but also the modifier for chitosan and contributed to the improvement of mechanical strength and adsorption performance of CTS/PAM gel. A batch of experiments were devoted to examine the performance of this gel as a function of adsorbent dosages, ion concentrations, adsorption time, initial pH, ionic strength, and recyclability test. In addition, practical industrial effluent was used to demonstrate the application of CTS/PAM gel. Some tests like Fourier transform infrared (FTIR) and X-ray photoelectron spectroscopy (XPS) were used to analyze the adsorption mechanism. Remarkably, the adsorption–regeneration–reuse treatment process used in this study promotes almost “zero” residue and can avoid the possibility of secondary pollution and reduce the operation and maintenance costs. The experimental performances demonstrated that CTS/PAM gel is an efficient, renewable, and sustainable promising adsorbent for heavy metal ions removal.

MATERIALS AND METHODS

Materials. Chitosan powder (deacetylation: 95%) was purchased from Aladdin Chemistry Co., Ltd. Ethylenediaminetetra-acetic acid (EDTA) and acrylamide were purchased from Sinopharm Chemical Reagent Co., Ltd. Potassium persulfate (KPS, AR) and *N,N*-

methylenebis(acrylamide) (MBA, AR) were provided by Shanghai Xitang Biotechnology Co., Ltd., China. All the chemicals were used as received. The industrial effluent was provided by Shuikoushan smelting plant located in Hengyang, Hunan province, China. All aqueous solutions were prepared with deionized water.

Preparation of CTS/PAM Gel. First, about 0.5 g of chitosan was dissolved in 8 mL of 1% (v/v) acetic acid solution to form solution A. Then, 1.0 g acrylamide, 0.3 mol % KPS (initiator for polyacrylamide), 1 mol % MBA (cross-linker) were added to 2 mL deionized water to form solution B. The solution A and solution B were mixed together and stirred at room temperature until homogeneous. The obtained sol was bubbled and injected into a 5 mm height cylinder molds with a diameter of 12 mm and these filled molds were presented in a forced convection oven for 2 h at 60 °C to complete the gelation process. Then the formed gel was immersed into 20 mL dimethyl sulfoxide contained 1.5 g EDTA anhydride synthesized according to Tülü and Geckeler²⁷ at 60 °C for 10 h. The obtained gel was thorough rinsed with ethanol and deionized water several times to remove unreacted reagents, and then drying to constant weight. Scheme 1 represents the formation of CTS/PAM gel.

Characterizations. Scanning electron microscopy (SEM) studies were performed on a FEI QUANTA 200 environmental scanning electron microscope. The thermogravimetric analysis (TGA) was measured under a nitrogen atmosphere with a TG/DTA7300 from room temperature to 700 °C with heating rate of 10 °C/min. The functional groups of samples were detected using a Fourier transform infrared Nicolet 5700 spectrophotometer (American). The surface chemistry of adsorbents during the preparation and adsorption process were determined by X-ray photoelectron spectroscopy (XPS, K-Alpha 1063, Thermo Fisher Scientific, England). Compression tests of the CTS/PAM gel were performed on a universal testing machine (HZ-1007C, Hengzhun, China). Swelling ratio of the DN gel was calculated as $SR = (W_s - W_d)/W_d$, moisture content of the swollen gel was calculated as $(W_s - W_d)/W_s \times 100\%$, where W_s and W_d are the weight of fully swollen and dry samples, respectively. The UV–vis spectra were conducted on a UV/vis/NIR spectrophotometer (UV-3600 Plus, Shimadzu). The pH values at the point of zero charge (pH_{PZC}) of the gel were measured by ΔpH drift method in a series of 0.01 M NaCl aqueous with different initial pH.

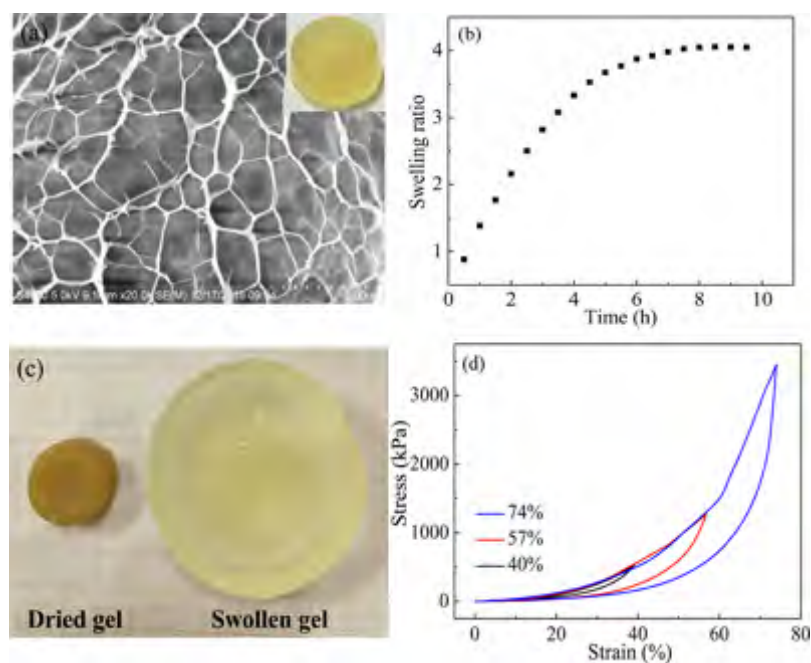


Figure 1. (a) SEM image of freeze-dried CTS/PAM gel. (inset) Raw gel. (b) Swelling ratio of CTS/PAM gel. (c) Photographs of dried and swollen CTS/PAM gel. (d) Typical consecutive loading–unloading curves of CTS/PAM gel with different compressive strain.

Batch Sorption of Heavy Metals. Analytical grade $\text{Cu}(\text{NO}_3)_2$, $\text{Cd}(\text{NO}_3)_2$ and $\text{Pb}(\text{NO}_3)_2$ were employed to prepare the $\text{Cu}(\text{II})$, $\text{Cd}(\text{II})$, and $\text{Pb}(\text{II})$ stock solutions. The pH values of the solution were adjusted by 0.1 M HCl or NaOH solutions. The sorbent dosage was calculated by the weight of dry hydrogel, and the gel was swollen with deionized water before adsorption. The adsorption experiments were carried out in an incubator shaker (QYC2112, Fuma, Shanghai, China) with the desired temperature of 298 K and fixed rotate speed of 160 rpm. The residual metal concentrations after adsorption were monitored on an atomic absorption spectrophotometer (Z-2000, Hitachi, Japan). The spent adsorbent was eluted with 1 M HCl solution and regenerated with 0.1 M NaOH solution, further washed with deionized water until neutral condition. Then the refreshed gel could be used in the next cycle of adsorption experiment. Changes in sorption capacity were determined at every cycle. All the experiments were performed twice under identical condition where the relative errors of the data were within 5%.

Industrial Effluents Treatment. The CTS/PAM gel was used to remove metal ions in the practical industrial effluent from Shuikoushan smelting plant located in Hengyang, Hunan province, China. The concentrations of metal ions in the practical effluent were measured by an atomic absorption spectrophotometer (Z-2000, Hitachi, Japan).

RESULTS AND DISCUSSION

Characterization. The SEM image of the freeze-dried CTS/PAM gel is shown in Figure 1a. It can be seen from the picture that the material possesses a highly interconnected macroporous network (the light part represents the wall and the gray part represents the pore) and high density of cross-links, which are the typical morphological features of DN hydrogels. The high density of cross-links can provide this gel with great mechanical strength.²⁸ Moreover, this porous structure is beneficial for the diffusion of heavy metal ions into the inside active site of the gel, and then would promote the adsorption of the heavy metal ions.

The swelling behavior of the CTS/PAM gel is shown in Figure 1b. The sample swelled as time going until reaching equilibrium at around 8 h with a swelling ratio of 4.0. The swollen CTS/PAM gel get a high moisture content of 80.2%

and without rupture at equilibrium state (Figure 1c). The appropriate swelling extent of CTS/PAM gel is largely due to the high density cross-links.²⁹ The high water content of it can promote metal ion mobility into the hydrogel which is beneficial to heavy metal adsorption.³⁰ Moreover, the UV–vis spectra (Figure S1a) of acrylamide aqueous and soaking solution of CTS/PAM gel in deionized water show that PAM did not dissolve and leach from the gel network.

Figure 1d shows the compressive nominal stress–strain curves for CTS/PAM gel. It can be seen that the loading curves toward a higher strain (74%) overlap the previous unloading curves (40% and 57%). After experiencing a certain loading stress of 3.5 MPa at $\epsilon = 74\%$, the CTS/PAM gel recovered to its original shape almost completely after unloading the stress. The high mechanic strength of CTS/PAM gel is attributable to the highly interconnected DN structure, which enable the synergistic energy dissipation and effective relaxation of locally applied stress.^{31,32}

Figure S1b shows the FTIR spectra of the CTS, pristine CTS/PAM gel, and CTS/PAM gel. All spectra exhibited broad and strong peaks in the range of $3500\text{--}3200\text{ cm}^{-1}$ due to the O–H stretching of the carbohydrate ring overlapping the N–H stretching vibration. The main signals in the chitosan are the saccharide ring signs of chitosan (1030 , 1116 , 1160 cm^{-1}), the vibrations of amide I (1650 cm^{-1}) and amide II (1591 cm^{-1}).³³ For the pristine CTS/PAM gel, a new peak at 3183 cm^{-1} occurred, representing the amide N–H stretching vibration. The vibrations of amide I and amide II are overlapped by a sharp band at 1646 cm^{-1} , which corresponds to the amide C=O stretching vibration.³⁴ For the CTS/PAM gel, the peaks of saccharide ring signs are overlapped by a sharp band at 1113 cm^{-1} , which can be assigned to the C–O stretching vibration of carboxylic acids. The peak at 1591 cm^{-1} (N–H bending vibration) disappeared, suggesting the successful grafting of EDTA onto the amino groups of chitosan.³⁵ This is consistent with the result in the calculation of carboxyl group on the CTS/PAM gel (Table S1).

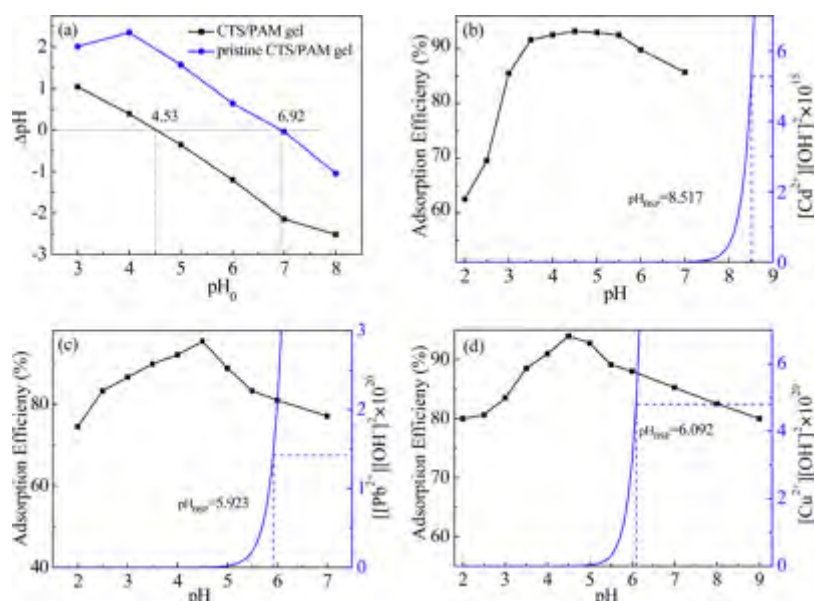


Figure 2. (a) Measurement of pH_{PZC} of CTS/PAM gels by ΔpH drift method, effect of pH on (b) Cd(II) ($C_0 = 55$ mg/L), (c) Pb(II) ($C_0 = 42$ mg/L), and (d) Cu(II) ($C_0 = 20$ mg/L) sorption on CTS/PAM gel, $T = 298$ K, $m/V = 1$ g/L. pH_{BSP} is the pH of bulk solution precipitation for the metal ion at the total metal concentration employed.

The thermogravimetric analyses (TGA) and the differential thermogravimetric data (DTG) curves of the CTS/PAM gels are shown in Figure S1c. The first DTG peak at 235.5 and 210.1 °C for CTS/PAM gel and the pristine one, respectively, is due to the loss of moisture.³⁶ The DTG peaks of pristine CTS/PAM gel at 313.1 and 370.0 °C are attributed to the depolymerization of chitosan chains and polyacrylamide network,^{37,38} respectively. After the modification with EDTA, the DTG peak at 313.1 °C disappeared. This is probably attributed to the enhanced thermostability of chitosan network that resulted from the cross-link between EDTA and chitosan.³⁹ The DTG peak at 362.8 °C is due to the pyrolysis of chitosan and polyacrylamide network. It can be concluded that the thermostability of these two gels displays the possibility for using as practical adsorbent.

After the modification, the zero-point value (pH_{PZC}) of CTS/PAM gel decreased from 6.92 to 4.53, suggesting the successful grafting of EDTA (Figure 2a). The final solution pH value increased with increasing initial pH at the point of $\text{pH} < \text{pH}_{\text{PZC}}$ because the attraction of CTS/PAM gels to H^+ , leading to the decrease in the number of protons. On the contrary, when $\text{pH} > \text{pH}_{\text{PZC}}$, the ΔpH kept negative value with increasing initial pH. This phenomenon probably due to the decline of concentration of OH^- in aqueous resulted from the affinity CTS/PAM gels showed to the negatively charged OH^- .

Effect of pH. The solution pH can simultaneously affect metal ion speciation in the solution and physicochemical nature of adsorbent.⁴⁰ The effect of initial solution pH on the uptake of Cd(II), Pb(II), and Cu(II) by CTS/PAM gel were investigated and the results are displayed in Figure 2b, c, and d, respectively. It can be seen that adsorption efficiency of metal ions increased upon increasing the solution up to pH 4.5 and then decreased. These results are opposite to the expectation from the zero-point value study of CTS/PAM gel. The relatively low adsorption efficiency at $\text{pH} < 2.5$ can be attributed to the competition of large amount of H^+ or H_3O^+ ions in the solution with metal ions.⁴¹ The significant rise in removal efficiency at pH ranging from 2.5 to 4.5 can be due to

the reduction amount of H^+ , resulting a weakened competition between H^+ and metal ions. With the further increasing pH, the removal efficiency of heavy metal ions decreased slightly. According to the previous discussion of pH_{PZC} , the CTS/PAM gel got an affinity to the negatively charged OH^- at the point of $\text{pH} > \text{pH}_{\text{PZC}}$. As we known, the concentration of OH^- increased with the increasing solution pH. The improvement of adsorbate affinity to the negatively charged OH^- resulted from the plenty of OH^- can directly reduce the adsorption ability of CTS/PAM gel to the positively charged heavy metal ions. Noticeably, the CTS/PAM gel exhibits a satisfactory adsorption performance of these three metal ions (more than 80% removal efficiency) during the neutral environment. The strong pH dependent adsorption suggests that the interaction between metal ions and adsorbent cannot be simply explained through an electrostatic interaction.^{42,43}

Effect of Ionic Strength. In this study, competitive sorption experiments were performed with Cd(II), Cu(II), and Pb(II) in the presence K(I), Na(I), Mg(II), and Ca(II). Figure S2 shows the removal performance of Cd(II), Cu(II), and Pb(II) by CTS/PAM gel in the presence of different concentration of cations (co-ion/heavy metal ion molar ratio ranging from 20 to 120). The removal efficiency of heavy metal ion reduced with the presence of interference ions, which compete for the same active sites of the adsorbent.⁴⁴ At the molar ratio of 120, the removal efficiency of Cd(II) (Figure S2a) decreased from 98.86% to 85.88%, 84.31%, 83.13%, and 68.62% in the presence of K(I), Na(I), Mg(II), and Ca(II), while that for Pb(II) (Figure S2b) changed from 98.09% to 85.04%, 80.65%, 79.10%, and 75.16%, respectively. Compared to Cd(II) and Pb(II), lesser difference exists in the removal efficiency of Cu(II) (Figure S2c). These results demonstrate that the adsorption of heavy metal ions are affected by the four co-ions at high concentration. In addition, the inhibitory effect of these co-ions on the removal of Cd(II), Cu(II), and Pb(II), follow this order: $\text{Ca(II)} > \text{Mg(II)} > \text{Na(I)} > \text{K(I)}$. This is consistent with the formation constant order of the metal ions

with EDTA:⁴⁵ Cu(II) > Pb(II) > Cd(II) > Ca(II) > Mg(II) > Na(I) > K(I).

Sorption Kinetics. The adsorption kinetics of metal ions by CTS/PAM gel was investigated and the results are depicted in Figure 3. About 70% of total Cd(II), Cu(II), and Pb(II)

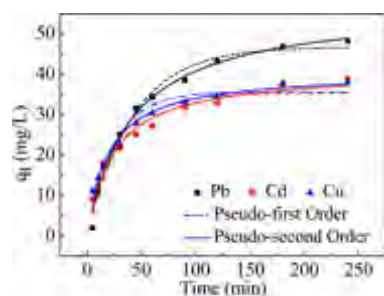


Figure 3. Time-dependent sorption on CTS/PAM gel of Cd(II) (pH = 6, $C_0 = 40$ mg/L), Pb(II) (pH = 5, $C_0 = 50$ mg/L), and Cu(II) (pH = 5, $C_0 = 40$ mg/L), $T = 298$ K, $m/V = 1$ g/L.

sorption on CTS/PAM gel rapidly occurs within 50 min, followed by a relatively slow process achieving the sorption equilibrium at about 170 min. The rapid adsorption is attributable to the three-dimensional loose and porous structure and its excellent water penetration, which can provide heavy metal ions with easier access to the adsorption sites. In this study, pseudo-first-order and pseudo-second-order models were used to analyze the sorption rate of heavy metal ions on CTS/PAM. The parameter values and the correlation coefficients for each system are calculated and presented in Table 1. It is found that the correlation coefficients of the modeled pseudo-second-order by experiment data (0.971, 0.981, and 0.987 for Cd(II), Cu(II), and Pb(II), respectively) are larger than those of the modeled pseudo-first-order (0.906, 0.927, and 0.983 for Cd(II), Cu(II), and Pb(II), respectively). This proves that the sorption kinetics of metal ions adsorption are well-described by pseudo-second-order rate equation. From a comparison of the rate constant k_2 and metal sorbed q_e , a reverse order is obtained. Hence, it can be suggested that the rate-determining step of heavy metal ions onto CTS/PAM gel might be ion-exchange interactions between metal ions and carboxyl groups.⁴⁶

Sorption Isotherms and Thermodynamics. Adsorption isotherms of Cd(II), Cu(II), and Pb(II) on CTS/PAM gel were obtained at pH 6.0, 5.0, and 5.0, respectively. Figure 4a shows the effect of adsorbent dosages on the adsorption of Cd(II), Cu(II), and Pb(II) at low concentration. Removal efficiency of all ions increased first and then remained unchanged with increasing adsorbent dosage, once the optimum dosage (400, 400, and 200 mg/L for Cd(II), Cu(II), and Pb(II), respectively) is reached. The removal efficiency keeps unchanged after reaching the sorption equilibrium, since there are a set number of adsorption sites on adsorbents.⁴⁷

Figure 4b shows the adsorption isotherms of Cd(II), Cu(II) and Pb(II) on CTS/PAM gel at 298 K. For these three ions, removal amount increased with increasing initial ion concentration. The experimental data are nonlinear fitted by the Langmuir and Freundlich isotherm models, and the parameters and correlation coefficients (R^2) are listed in Table 2. It appears that adsorbate–adsorbent system can be better explained by the Langmuir model, in accordance with the correlation coefficient results (0.993 for Pb(II), 0.976 for Cu(II), and 0.943 for Cd(II)). According to the Freundlich study, the k_F parameter is different for each gel–metal ion and the n values are higher than 1, which confirmed that the sorption process might have taken place through electrostatic interaction, ion-exchange or a combined mechanism.⁴⁸ Table S2 lists the heavy metal adsorption capacities of CTS/PAM gel and some other adsorbents reported recent years. The maximum sorption capacities of Cd(II), Cu(II), and Pb(II) on CTS/PAM gel are calculated to be 86.00, 99.44, and 138.41 mg/g, respectively, by the Langmuir isotherm model. It is found that the sorption capacities of heavy metal ions on CTS/PAM gel are comparatively high.

The Dubinin–Radushkevich (DR) isotherm was applied to estimate the adsorption energy. Figure S3 shows the adsorption isotherm data fitted by the DR isotherm. According to DR isotherm analysis, the values of average free energy (E) are 13.82, 12.39, and 12.60 kJ/mol for Cd(II), Pb(II), and Cu(II) sorption (Table 2). These values are between 8 and 16 kJ/mol, showing that ion-exchange taken place in the adsorption process.⁴⁹ Meanwhile, the negative values of ΔG^0 and the positive values ΔH^0 and ΔS^0 (Table 3) calculated from van't Hoff equation indicate that the sorption of heavy metal ions on the CTS/PAM gel is spontaneous and endothermic with high affinity under the experimental conditions.⁵⁰

Treatment of Actual Industrial Effluent. The initial pH value of the industrial effluent was measured as 2.8 and adjusted to 5.0 ± 0.1 by 0.1 M NaOH solution before being treated with CTS/PAM gel. The main heavy metal species and experimental data are summarized in Table 4. There are several kinds of main heavy metal ions exist such as Cd(II), Pb(II), Cu(II), Zn(II), Ni(II), and Mn(II) with initial concentrations of 4.75, 24.75, 8.75, 389.625, 1.875, and 18.75 mg/L, respectively, and the total concentration of heavy metal ions reaches 448.5 mg/L. After being treated with 1 g/L adsorbent, the removal efficiency of Pb(II) and Cu(II) reach 86% and 91%, respectively. Apparently, the removal efficiency increased with increasing adsorbent dosage. With the largest adsorbent dosage (8 g/L), residue concentration of Zn(II) and Mn(II) are 4.75 and 0.07 mg/L, respectively. It is easy to conclude that the changes in removal efficiencies are dependent on the gel dosage. This gel is proved to be a potential and efficient adsorbent for treating practical wastewater contains heavy metals.

Selective Adsorption and Recyclability Test. A mixed solution of metal ions containing Pb(II), Cu(II), Cd(II), Zn(II), Mn(II), and Ni(II) was prepared, the concentration of

Table 1. Constants for the Kinetic Sorption Data Using Different Sorption Models

metal ions	Q_e (mg/g)	pseudo-first-order			pseudo-second-order		
		k_1 (L/min)	$Q_{e,cal}$ (mg/g)	R^2	k_2 (g/(mg min))	$Q_{e,cal}$ (mg/g)	R^2
Cd(II)	38.96	0.0337	35.27	0.906	0.00102	40.82	0.971
Pb(II)	48.31	0.0239	46.74	0.983	0.00044	56.94	0.987
Cu(II)	38.05	0.0398	35.64	0.927	0.00125	40.68	0.981

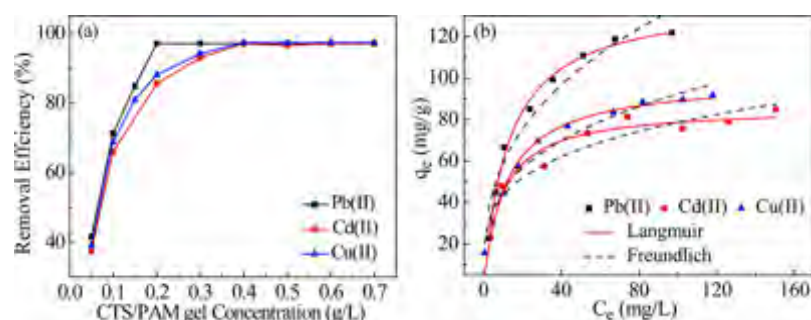


Figure 4. Adsorption of Cd(II) (pH = 6), Cu(II) (pH = 5), and Pb(II) (pH = 5) onto CTS/PAM gel. (a) Different adsorbent dosages with a same initial concentration 20 mg/L of each ion. (b) Adsorption isotherms of each ion, $t_{\text{contact}} = 6$ h, $m/V = 1$ g/L.

Table 2. Parameters of Isotherm Models

metals	Langmuir			Freundlich			Dubinin–Radushkevich		
	Q_m (mg/L)	K_L (L/mg)	R^2	K_F ($\text{mg}^{1-n} \text{L}^n/\text{g}$)	n_F	R^2	k (mol^2/kJ^2)	E (kJ/mol)	R^2
Cd(II)	85.00	0.106	0.943	23.88	3.864	0.893	2.617×10^{-9}	13.82	0.917
Pb(II)	138.41	0.077	0.993	25.73	2.789	0.940	3.255×10^{-9}	12.39	0.961
Cu(II)	99.44	0.084	0.976	22.78	3.293	0.968	3.151×10^{-9}	12.60	0.979

Table 3. Values of Thermodynamic Parameters for Metal Ion Sorption

metals	T (K)	ΔG^0 (kJ/mol)	ΔS^0 (J/(mol K))	ΔH^0 (kJ/mol)
Cd(II)	293	-4.713	45.92	8.74
	298	-4.937		
	303	-5.172		
Pb(II)	293	-4.797	122.77	31.22
	298	-5.277		
	303	-6.028		
Cu(II)	293	-5.125	185.84	49.40
	298	-5.809		
	303	-6.989		

all heavy metal ions was set to 50 mg/L, for selective adsorption test. Figure 5a shows that the uptake of Cu(II) is higher than other heavy metals, and the removal efficiency order is Cu(II) > Pb(II) > Ni(II) > Cd(II) > Zn(II) > Mn(II). Nevertheless, the order of formation constants of these six ions with EDTA⁴⁵ can be shown as Cu(II) > Ni(II) > Pb(II) > Cd(II) = Zn(II) > Mn(II). Little discrepancy exists between these two orders, which is probably caused by the competition and electrostatic repulsion among metal ions. The distribution ratios and selectivity coefficients (see Supporting Information) of Cu(II) toward other metal ions by CTS/PAM gel are displayed in Table S3. The relative selectivity coefficients of

CTS/PAM gel for each specific metal ion are far greater than 1, suggesting its priority on the sorption of Cu(II) and ability to remove other metal species in a mixed solution.

To demonstrate the renewability and reusability of CTS/PAM gel, 1 M HCl eluent was used to desorb the heavy metal ions which adsorbed onto the gel, then desorbed adsorbent was regenerated by 0.1 M NaOH solution and deionized water. Figure 5b shows the removal efficiency of Cd(II), Cu(II), and Pb(II) in each cycle. The removal efficiencies are 93.7%, 94.1%, and 91.4% for Cd(II), Cu(II), and Pb(II) at the first cycle, respectively. Some loss (within 3% decline) of heavy metal ions removal efficiencies is observed for the regenerated CTS/PAM gel after 5 cycles, meaning the good reusability of this adsorbent. Additionally, the CTS/PAM gel can be separated directly from aqueous solution without obviously adsorbent loss.

Adsorption Mechanism. It has been discussed that the interactions between heavy metal ions and adsorbent might be taken place through ion exchange process predominantly at effect of pH, kinetic experiment, and adsorption isotherm analysis. In order to further understand the mechanism of heavy metal sorption on CTS/PAM gel, the functional groups, and chemical status of adsorbent before and after saturate sorption of Cd(II) were examined by FTIR and XPS scans, respectively. XPS has often been used to identify the mechanism of heavy metal sorption because the interaction between metal ion and

Table 4. Characteristics of Metal Ion Concentration of Industrial Effluent before and after Being Treated with Different Adsorbent Dosages

adsorbent dosage (g/L)	pH	metal ions concentration (mg/L)					
		Cd(II)	Pb(II)	Cu(II)	Zn(II)	Ni(II)	Mn(II)
0	2.8	4.750	24.75	8.750	389.625	1.875	18.75
1	5.0	4.100	3.425	0.725	122.600	1.350	12.25
2	5.0	2.200	2.375	0.100	117.700	0.875	10.75
3	5.0	1.350	0.725	0.050	111.975	0.550	9.25
4	5.0	1.125	0.125	0.025	96.925	0.325	7.25
5	5.0	0.350	0.075	0.022	81.850	0.100	5.00
6	5.0	0.075	0.050	<0.01	65.575	<0.01	3.02
8	5.0	<0.01	<0.01	<0.01	4.75	<0.01	0.07

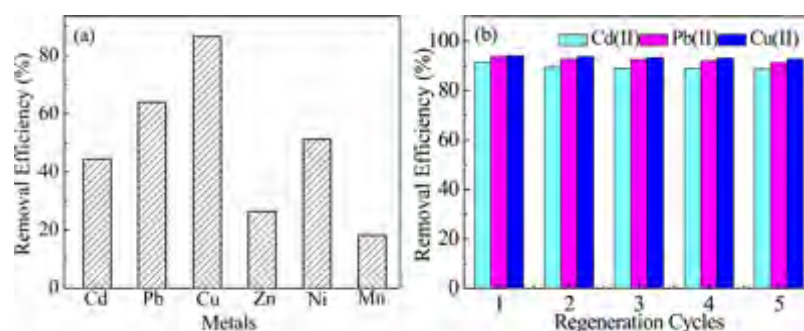


Figure 5. (a) Metal ions removal on CTS/PAM gel from a mixed solution of metal ions ($C_{\text{initial}} = 50 \text{ mg/L}$, $\text{pH} = 5.0$, $t_{\text{contact}} = 6 \text{ h}$, $T = 298 \text{ K}$, $m/V = 1 \text{ g/L}$). (b) Cd(II) ($\text{pH} = 6$, $C_0 = 50 \text{ mg/L}$), Pb(II) ($\text{pH} = 5$, $C_0 = 60 \text{ mg/L}$), and Cu(II) ($\text{pH} = 5$, $C_0 = 45 \text{ mg/L}$) removal efficiency from solution by CTS/PAM gel during five regeneration cycles.

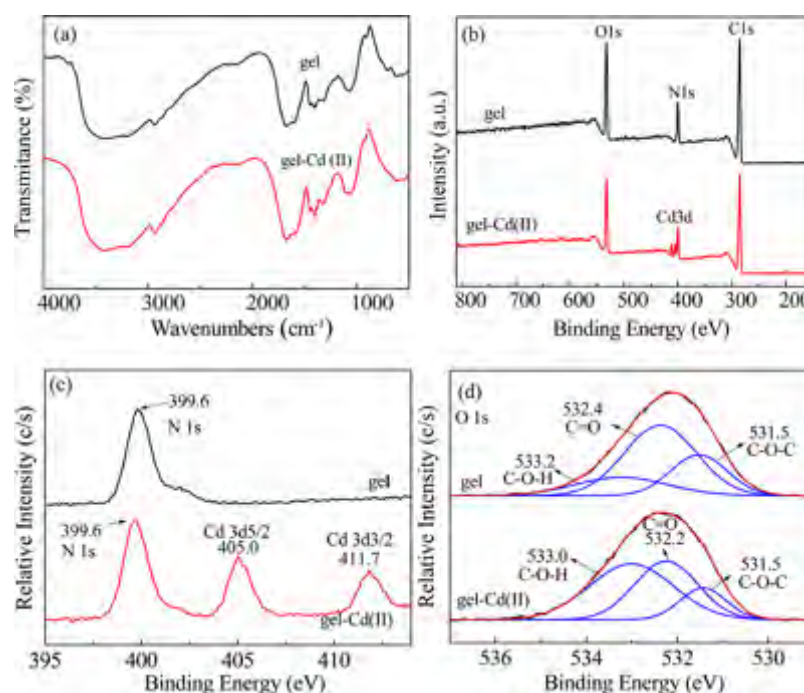


Figure 6. (a) FTIR spectra, (b) total survey scans of XPS spectra, (c) N 1s and Cd 3d, and (d) O 1s of CTS/PAM gel before and after adsorption of Cd(II).

functional groups may change the distribution of the electrons around the corresponding atoms.⁵¹

The FTIR spectra are shown in Figure 6a. It can be seen the corresponding bands of CTS/PAM gel remaining unchanged after the adsorption of Cd(II), indicating the functional groups were not changed. It seems that chemical sorption was not occurred between Cd(II) and carboxylate groups during the adsorption process.⁵² Figure 6b gives an overview of the bonding environment of the two samples analyzed by the XPS survey scans. Three remarkable intense peaks (O 1s, N 1s, C 1s) are displayed in the XPS pattern of CTS/PAM gel. Apparently, two new peaks appeared in the XPS spectra of gel-Cd(II) suggesting the successful attachment of Cd(II) onto adsorbent. As shown in Figure 6c, the N 1s XPS peaks of CTS/PAM gel can be fitted by only one peak at 399.6 eV for the nitrogen in the amide groups, and kept unchanged after the adsorption of Cd(II). It is due to the lone pair of electrons of nitrogen atom in amide group were occupied, and the nitrogen atom was unlikely to donate the lone pairs to metal ions. In Figure 6c, two group peaks in the XPS spectra of gel-Cd(II) at

405.0 and 411.7 eV, assigning to Cd 3d_{5/2} and Cd 3d_{3/2}, respectively, are same as the binding energy of Cd 3d_{5/2} and Cd 3d_{3/2} in ionic form. The result demonstrating that Cd(II) is not in coordination form but ionic form.⁵³ The O 1s spectrum of the CTS/PAM gel in Figure 6d can be fitted by three peaks at around 533.2, 532.4, and 531.5 eV assigned to O 1s in C-O-H, C=O, and C-O-C.⁵⁴ After the adsorption of Cd(II), no change of the peak at 531.5 eV can be observed, while little discrepancy happened to the peaks of C-O-H and C=O (shifted to 533.0 and 532.2 eV, respectively), indicating the carboxylate groups on the surface of CTS/PAM gel are involved in the adsorption process. Moreover, the changes in binding energy illustrating that the interaction mechanism between carboxylate groups and Cd(II) is not complexation.⁵⁵ Based on the above discussion, the adsorption mechanism can be concluded to ion exchange interactions by metal ions with carboxylate groups.

CONCLUSIONS

Double network hydrogels represent a new class of sustainable materials with recognized potential in heavy metal removal. It is found that this adsorption process could be described well by the pseudo-second-order kinetic and Langmuir isotherm model. Besides satisfactory adsorption ability, CTS/PAM gel possesses many merits such as low cost, excellent mechanical strength, rapid separation, and outstanding reusability which are important properties for practical application of adsorbent. Additionally, this gel shows a good performance in practical wastewater treatment. It is expected that CTS/PAM gel will have potentially wide application in heavy metal pollutants removal from aquatic systems.

ASSOCIATED CONTENT

Supporting Information

The Supporting Information is available free of charge on the ACS Publications website at DOI: 10.1021/acssuschemeng.6b02181.

Further details including the determination of carboxyl content, the introduction of kinetic and adsorption models, selective adsorption, UV-vis spectra, FTIR spectra, TGA curves, figures of cations strength effect, and tables of sorption capacities comparison with other sorbents and selective adsorption (PDF)

AUTHOR INFORMATION

Corresponding Author

*Tel./Fax: +86-731-88823805. E-mail address: yt_liu@hnu.edu.cn (Y.L.).

ORCID

Yutang Liu: 0000-0002-4975-364X

Notes

The authors declare no competing financial interest.

ACKNOWLEDGMENTS

This work was supported by the National Natural Science Foundation of China (51238002, 51378187, and 51478171), Hunan Provincial Natural Science Foundation of China (14JJ1015), and Program for Innovation Research Team in University (IRT1238).

REFERENCES

- (1) Vorosmarty, C. J.; McIntyre, P. B.; Gessner, M. O.; Dudgeon, D.; Prusevich, A.; Green, P.; Glidden, S.; Bunn, S. E.; Sullivan, C. A.; Liermann, C. R.; Davies, P. M. Global threats to human water security and river biodiversity. *Nature* **2010**, *467*, 555–561.
- (2) Oki, T.; Kanae, S. Global hydrological cycles and world water resources. *Science* **2006**, *313*, 1068–1072.
- (3) Chen, Q. Y.; Luo, Z.; Hills, C.; Xue, G.; Tyrer, M. Precipitation of heavy metals from wastewater using simulated flue gas: sequent additions of fly ash, lime and carbon dioxide. *Water Res.* **2009**, *43*, 2605–2614.
- (4) Yang, G. X.; Jiang, H. Amino modification of biochar for enhanced adsorption of copper ions from synthetic wastewater. *Water Res.* **2014**, *48*, 396–405.
- (5) Cao, L. T. T.; Koda, H.; Abe, K.; Imachi, H.; Aoi, Y.; Kindaichi, T.; Ozaki, T.; Ohashi, A. Biological oxidation of Mn(II) coupled with nitrification for removal and recovery of minor metals by downflow hanging sponge reactor. *Water Res.* **2015**, *68*, 545–553.
- (6) Thong, Z. W.; Han, G.; Cui, Y.; Gao, J.; Chung, T. S.; Chan, S. Y.; Wei, S. Novel nanofiltration membranes consisting of a sulfonated

pentablock copolymer rejection layer for heavy metal removal. *Environ. Sci. Technol.* **2014**, *48*, 13880–13887.

- (7) Shan, C.; Ma, Z. Y.; Tong, M. P.; Ni, J. R. Removal of Hg(II) by poly(1-vinylimidazole)-grafted Fe₃O₄@SiO₂ magnetic nanoparticles. *Water Res.* **2015**, *69*, 252–260.

- (8) Wang, J. L.; Chen, C. Chitosan-based biosorbents: modification and application for biosorption of heavy metals and radionuclides. *Bioresour. Technol.* **2014**, *160*, 129–141.

- (9) Burtch, N. C.; Jasuja, H.; Walton, K. S. Water stability and adsorption in metal-organic frameworks. *Chem. Rev.* **2014**, *114*, 10575–10612.

- (10) Ali, I. New generation adsorbents for water treatment. *Chem. Rev.* **2012**, *112* (10), 5073–5091.

- (11) Calvert, P. Hydrogels for Soft Machines. *Adv. Mater.* **2009**, *21*, 743–756.

- (12) Seliktar, D. Designing cell-compatible hydrogels for biomedical applications. *Science* **2012**, *336*, 1124–1128.

- (13) Sun, J. Y.; Zhao, X. H.; Illeperuma, W. R. K.; Chaudhuri, O.; Oh, K. H.; Mooney, D. J.; Vlassak, J. J.; Suo, Z. G. Highly stretchable and tough hydrogels. *Nature* **2012**, *489*, 133–136.

- (14) Zhang, Y. Y.; Li, Y. M.; Liu, W. G. Dipole-Dipole and H-Bonding Interactions Significantly Enhance the Multifaceted Mechanical Properties of Thermoresponsive Shape Memory Hydrogels. *Adv. Funct. Mater.* **2015**, *25*, 471–480.

- (15) Chen, Q.; Zhu, L.; Huang, L. N.; Chen, H.; Xu, K.; Tan, Y.; Wang, P. X.; Zheng, J. Fracture of the Physically Cross-Linked First Network in Hybrid Double Network Hydrogels. *Macromolecules* **2014**, *47*, 2140–2148.

- (16) Thakur, V. K.; Thakur, M. K. Recent Advances in Graft Copolymerization and Applications of Chitosan: A Review. *ACS Sustainable Chem. Eng.* **2014**, *2*, 2637–2652.

- (17) Oladipo, A. A.; Gazi, M. Hydroxyl-enhanced magnetic chitosan microbeads for boron adsorption: Parameter optimization and selectivity in saline water. *React. Funct. Polym.* **2016**, *109*, 23–32.

- (18) Duan, J. F.; Liua, Y. D.; Liua, L. J.; Jianga, J. X.; Lia, J. Z. Double-Network Carboxymethyl Chitosan Grafting Polyacrylamide/Alginate Hydrogel Compositions Adapted to Achieve High Stretchable Properties. *J. Mol. Genet. Med.* **2015**, *9*, 177.

- (19) Bao, D. S.; Chen, M. J.; Wang, H. Y.; Wang, J. F.; Liu, C. F.; Sun, R. C. Preparation and characterization of double crosslinked hydrogel films from carboxymethylchitosan and carboxymethylcellulose. *Carbohydr. Polym.* **2014**, *110*, 113–120.

- (20) Zhao, F. P.; Tang, W. Z.; Zhao, D. B.; Meng, Y.; Yin, D. L.; Sillanpää, M. Adsorption kinetics, isotherms and mechanisms of Cd(II), Pb(II), Co(II) and Ni(II) by a modified magnetic polyacrylamide microcomposite adsorbent. *J. Water Process. Eng.* **2014**, *4*, 47–57.

- (21) Oladipo, A. A.; Gazi, M.; Saber-Samandari, S. Adsorption of anthraquinone dye onto eco-friendly semi-IPN biocomposite hydrogel: Equilibrium isotherms, kinetic studies and optimization. *J. Taiwan Inst. Chem. Eng.* **2014**, *45*, 653–664.

- (22) Ngwabebhoh, F. A.; Gazi, M.; Oladipo, A. A. Adsorptive removal of multi-azo dye from aqueous phase using a semi-IPN superabsorbent chitosan-starch hydrogel. *Chem. Eng. Res. Des.* **2016**, *112*, 274–288.

- (23) Oladipo, A. A.; Gazi, M. Microwaves initiated synthesis of activated carbon-based composite hydrogel for simultaneous removal of copper(II) ions and direct red 80 dye: A multi-component adsorption system. *J. Taiwan Inst. Chem. Eng.* **2015**, *47*, 125–136.

- (24) Oladipo, A. A.; Gazi, M.; Yilmaz, E. Single and binary adsorption of azo and anthraquinone dyes by chitosan-based hydrogel: Selectivity factor and Box-Behnken process design. *Chem. Eng. Res. Des.* **2015**, *104*, 264–279.

- (25) Zhao, F. P.; Repo, E.; Sillanpää, M.; Meng, Y.; Yin, D. L.; Tang, W. Z. Green Synthesis of Magnetic EDTA- and/or DTPA-Cross-Linked Chitosan Adsorbents for Highly Efficient Removal of Metals. *Ind. Eng. Chem. Res.* **2015**, *54*, 1271–1281.

- (26) Hu, M.; Gu, X. Y.; Hu, Y.; Wang, T.; Huang, J.; Wang, C. Y. Low Chemically Cross-Linked PAM/C-Dot Hydrogel with Robust

ness and Superstretchability in Both As-Prepared and Swelling Equilibrium States. *Macromolecules* **2016**, *49*, 3174–3183.

(27) Tülü, M.; Geckeler, K. E. Synthesis and properties of hydrophilic polymers. Part 7. Preparation, characterization and metal complexation of carboxy-functional polyesters based on poly (ethylene glycol). *Polym. Int.* **1999**, *48*, 909–914.

(28) Kawano, S.; Kobayashi, D.; Taguchi, S.; Kunitake, M.; Nishimi, T. Construction of Continuous Porous Organogels, Hydrogels, and Bicontinuous Organo/Hydro Hybrid Gels from Bicontinuous Microemulsions. *Macromolecules* **2010**, *43*, 473–479.

(29) Cipriano, B. H.; Banik, S. J.; Sharma, R.; Rumore, D.; Hwang, W.; Briber, R. M.; Raghavan, S. R. Superabsorbent Hydrogels That Are Robust and Highly Stretchable. *Macromolecules* **2014**, *47*, 4445–4452.

(30) Chu, L.; Liu, C. B.; Zhou, G. Y.; Xu, R.; Tang, Y. H.; Zeng, Z. B.; Luo, S. L. A double network gel as low cost and easy recycle adsorbent: Highly efficient removal of Cd(II) and Pb(II) pollutants from wastewater. *J. Hazard. Mater.* **2015**, *300*, 153–160.

(31) Gong, J. P.; Katsuyama, Y.; Kurokawa, T.; Osada, Y. Double-network hydrogels with extremely high mechanical strength. *Adv. Mater.* **2003**, *15*, 1155–1158.

(32) Du, G. L.; Gao, G. R.; Hou, R. X.; Cheng, Y. J.; Chen, T.; Fu, J.; Fei, B. Tough and Fatigue Resistant Biomimetic Hydrogels of Interlaced Self-Assembled Conjugated Polymer Belts with a Polyelectrolyte Network. *Chem. Mater.* **2014**, *26*, 3522–3529.

(33) Lawrie, G.; Keen, I.; Drew, B.; Chandler-Temple, A.; Rintoul, L.; Fredericks, P.; Grøndahl, L. Interactions between alginate and chitosan biopolymers characterized using FTIR and XPS. *Biomacromolecules* **2007**, *8*, 2533–2541.

(34) Liu, R. Q.; Liang, S. M.; Tang, X. Z.; Yan, D.; Li, X. F.; Yu, Z. Z. Tough and highly stretchable graphene oxide/polyacrylamide nanocomposite hydrogels. *J. Mater. Chem.* **2012**, *22*, 14160–14167.

(35) Liu, Q.; Yang, B. C.; Zhang, L. J.; Huang, R. H. Adsorption of an anionic azo dye by cross-linked chitosan/bentonite composite. *Int. J. Biol. Macromol.* **2015**, *72*, 1129–1135.

(36) Huacai, G.; Wan, P.; Dengke, L. Graft copolymerization of chitosan with acrylic acid under microwave irradiation and its water absorbency. *Carbohydr. Polym.* **2006**, *66*, 372–378.

(37) Gao, X. Y.; Zhou, Y. S.; Ma, G. P.; Shi, S. Q.; Yang, D. Z.; Lu, F. M.; Nie, J. A water-soluble photocrosslinkable chitosan derivative prepared by Michael-addition reaction as a precursor for injectable hydrogel. *Carbohydr. Polym.* **2010**, *79*, 507–512.

(38) Yang, F.; Li, G.; He, Y. G.; Ren, F. X.; Wang, G. X. Synthesis, characterization, and applied properties of carboxymethyl cellulose and polyacrylamide graft copolymer. *Carbohydr. Polym.* **2009**, *78*, 95–99.

(39) Zhao, F. P.; Repo, E.; Yin, D. L.; Meng, Y.; Jafari, S.; Sillanpää, M. EDTA-Cross-Linked β -Cyclodextrin: An Environmentally Friendly Bifunctional Adsorbent for Simultaneous Adsorption of Metals and Cationic Dyes. *Environ. Sci. Technol.* **2015**, *49*, 10570–10580.

(40) Xu, R.; Zhou, G. Y.; Tang, Y. H.; Chu, L.; Liu, C. B.; Zeng, Z. B.; Luo, S. L. New double network hydrogel adsorbent: Highly efficient removal of Cd(II) and Mn(II) ions in aqueous solution. *Chem. Eng. J.* **2015**, *275*, 179–188.

(41) Zhao, F. P.; Repo, E.; Yin, D. L.; Sillanpää, M. E. T. Adsorption of Cd(II) and Pb(II) by a novel EGTA-modified chitosan material: Kinetics and isotherms. *J. Colloid Interface Sci.* **2013**, *409*, 174–182.

(42) Jin, L.; Bai, R. B. Mechanisms of lead adsorption on chitosan/PVA hydrogel beads. *Langmuir* **2002**, *18*, 9765–9770.

(43) Brown, P. A.; Gill, S. A.; Allen, S. J. Metal removal from wastewater using peat. *Water Res.* **2000**, *34*, 3907–3916.

(44) Huang, G. L.; Wang, D.; Ma, S. L.; Chen, J. L.; Jiang, L.; Wang, P. Y. A new, low-cost adsorbent: Preparation, characterization, and adsorption behavior of Pb(II) and Cu(II). *J. Colloid Interface Sci.* **2015**, *445*, 294–302.

(45) Harris, D. C. *Quantitative Chemical Analysis*, eighth ed.; Macmillan: New York, 2010.

(46) Reddad, Z.; Gerente, C.; Andres, Y.; Le Cloirec, P. Adsorption of several metal ions onto a low-cost biosorbent: kinetic and equilibrium studies. *Environ. Sci. Technol.* **2002**, *36*, 2067–2073.

(47) Huang, Y. X.; Keller, A. A. EDTA functionalized magnetic nanoparticle sorbents for cadmium and lead contaminated water treatment. *Water Res.* **2015**, *80*, 159–168.

(48) Paulino, A. T.; Guilherme, M. R.; Reis, A. V.; Tambourgi, E. B.; Nozaki, J.; Muniz, E. C. Capacity of adsorption of Pb²⁺ and Ni²⁺ from aqueous solutions by chitosan produced from silkworm chrysalides in different degrees of deacetylation. *J. Hazard. Mater.* **2007**, *147*, 139–147.

(49) Günay, A.; Arslankaya, E.; Tosun, I. Lead removal from aqueous solution by natural and pretreated clinoptilolite: adsorption equilibrium and kinetics. *J. Hazard. Mater.* **2007**, *146*, 362–371.

(50) Sun, Z. C.; Liu, Y. G.; Huang, Y. Q.; Tan, X. F.; Zeng, G. M.; Hu, X. J.; Yang, Z. Z. Fast adsorption of Cd²⁺ and Pb²⁺ by EGTA dianhydride (EGTAD) modified ramie fiber. *J. Colloid Interface Sci.* **2014**, *434*, 152–158.

(51) Deng, S. B.; Bai, R.; Chen, J. P. Aminated polyacrylonitrile fibers for lead and copper removal. *Langmuir* **2003**, *19*, 5058–5064.

(52) Kyzas, G. Z.; Sifaka, P. I.; Lambropoulou, D. A.; Lazaridis, N. K.; Bikiaris, D. N. Poly(itaconic acid)-grafted chitosan adsorbents with different cross-linking for Pb(II) and Cd(II) uptake. *Langmuir* **2014**, *30*, 120–131.

(53) Luo, S. L.; Li, X. J.; Chen, L.; Chen, J. L.; Wan, Y.; Liu, C. B. Layer-by-layer strategy for adsorption capacity fattening of endophytic bacterial biomass for highly effective removal of heavy metals. *Chem. Eng. J.* **2014**, *239*, 312–321.

(54) Huang, J.; Ye, M.; Qu, Y. Q.; Chu, L. F.; Chen, R.; He, Q. Z.; Xu, D. F. Pb (II) removal from aqueous media by EDTA-modified mesoporous silica SBA-15. *J. Colloid Interface Sci.* **2012**, *385*, 137–146.

(55) Zhou, G. Y.; Luo, J. M.; Liu, C. B.; Chu, L.; Ma, J. H.; Tang, Y. H.; Zeng, Z. B.; Luo, S. L. A highly efficient polyampholyte hydrogel sorbent based fixed-bed process for heavy metal removal in actual industrial effluent. *Water Res.* **2016**, *89*, 151–60.